jaxparrow: a Python package solving the cyclogeostrophic balance using a variational formulation

Victor E V Z DE ALMEIDA[1*], **Vadim BERTRAND**[1*], **Julien LE SOMMER**[1*], **and Emmanuel COSME**[1*]

1 Univsersité Grenoble Alpes, France * These authors contributed equally.

Summary

Sea Surface Height (SSH) variations measured by satellite altimeters are widely used to estimate Sea Surface Currents (SSC) in oceanographic operational or research applications. The geostrophic balance approximation, which relates the pressure gradient, the current velocity, and the Coriolis force, is commonly employed to estimate SSC from SSH. It is known that under some configurations, the centrifugial acceleration, disregarded in the geostrophic formulation, should be included to the balance, leading to the cyclogeostrophic balance approximation. In general, solving the cyclogeostrophic balance can not be done analytically and numerical methods are needed. However, (1) existing iterative approaches are known to diverge, and ad-hoc methods should be used to avoid local discontinuities; (2) well documented, and publicly available implementations are missing.

To overcome these limitations, we propose the Python package `jaxparrow`. `jaxparrow` formulates the cyclogeostrophic balance as a variational problem and solve it using a collection of well known optimizers. Its implementation heavily relies on JAX, the Python library bringing together automatic differentation and just-in-time compilation, and the growing ecosystem around it. `jaxparrow` can be used as a package for an easy integration to existing oceanographic pipelines, or as a standalone executable working directly with NetCDF files.

Statement of need

Sea Surface Currents (SSC) can be easily approximated from satellite altimetry observations of the Sea Surface Height (SSH) using the geostrophic balance. Geostrophy describes the balance between the pressure gradient force (indirectly observed via the SSH), and the Coriolis force. Geostrophic currents satisfy this equilibrium:

$$f\left(\vec{k} \times \vec{u}_g\right) = -g\nabla\eta, \tag{1}$$

where f is the Coriolis parameter, $\vec{k}$ the vertical unit vector, $\vec{u}_g$ the geostrophic velocity, g the gravity, and η the Sea Surface Height.

However, as discussed by Charney (1955), Bakun (2006), and Maximenko & Niiler (2006), geostrophy alone is not always sufficient to accurately estimate the SSC, and an advective term should be considered. For example, it has been shown by Penven et al. (2014) that, in the highly energetic Mozambique Channel, the geostrophic velocity can produce errors in the order of 30%. In these conditions, the centrifugal acceleration and the inertial effects of oceanic dynamics are no longer neglectable. To account for those forces, the advective term

---

37 $\vec{u} \cdot \nabla \vec{u}$ is added back to the balance. Considering a horizontal, stationary, and inviscid flow, the
38 momentum equation linking the currents velocity $\vec{u}$ with the SSH —through the geostrophic
39 velocity $\vec{u}_g$ from Equation 1— can be expressed as:

$$\vec{u}_c - \frac{\vec{k}}{f} \times (\vec{u}_c \cdot \nabla \vec{u}_c) = \vec{u}_g, \tag{2}$$

40 where $\vec{u}_c$ is the cyclogeostrophic velocity.

41 Ocean data and services providers, such as Copernicus Marine Environment Monitoring Service,
42 rely on the geostrophic balance. Cao et al. (2023) demonstrates that applying cyclogeostrophic
43 corrections to the global ocean over a 25-years period results in significantly different ocean
44 dynamics. As such, ocean products could greatly benefit from a robust and open estimation
45 method of cyclogeostrophic currents.

Numerical resolution of the cyclogeostrophic inverse problem

47 Because of the advective term $\vec{u}_c \cdot \nabla \vec{u}_c$, Equation 2 is nonlinear, and solving it analytically is
48 conceivable only in idealized scenarios, making numerical approaches essential. The current
49 state-of-the-art method to solve the cyclogeostrophic equation is the iterative formulation
50 introduced by Arnason et al. (1962) and Endlich (1961), which consists of reaching balance
51 using the following iterative scheme:

$$\vec{u}_c^{(n+1)} = \vec{u}_g + \frac{\vec{k}}{f} \times \left(\vec{u}_c^{(n)} \cdot \nabla \vec{u}_c^{(n)} \right), \tag{3}$$

52 with $\vec{u}_c^{(0)} = \vec{u}_g$. This approach is known to diverge since Arnason et al. (1962), and in practice
53 (Ioannou et al., 2019; Penven et al., 2014) the residual $res = |\vec{u}_c^{(n+1)} - \vec{u}_c^{(n)}|$ is used to control
54 point by point the iteration process. The iteration locally stops when the point residual is
55 below 0.01 m/s or starts to increase.

56 To avoid the local divergence issue of the iterative process, and its ad-hoc control, we propose
57 to formulate the cyclogeostrophy as the variational problem:

$$J(\vec{u}_c) = \left\| \vec{u}_c - \frac{\vec{k}}{f} \times (\vec{u}_c \cdot \nabla \vec{u}_c) - \vec{u}_g \right\|^2, \tag{4}$$

58 where $\|.\|$ is the discrete L^2 norm. Thanks to JAX (Bradbury et al., 2021) automatic
59 differentiation capabilities, ∇J is numerically available, and the cyclogeostrophic currents are
60 estimated by minimizing Equation 4 using a gradient-based optimizer, with $\vec{u}_c^{(0)} = \vec{u}_g$ as initial
61 guess.

Application to the Alboran sea

63 The Alboran sea is an energetic area of the Mediterannean sea. We demonstrate below the
64 need to consider cyclogeostrophy in this region, and in particular the benefit of the variational
65 formulation implemented in `jaxparrow`. The data and results presented here can be found in
66 the Alboran sea notebook hosted on GitHub.

67 We use SSH and SSC from the eNATL60 configuration (Brodeau et al., 2020; Uchida et al.,
68 2022) of the state-of-the-art NEMO ocean circulation model (Madec et al., 2022) as reference
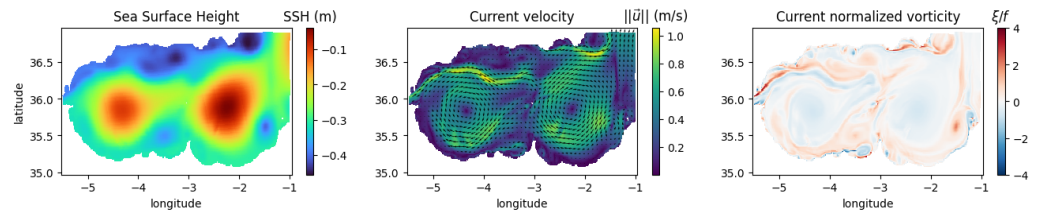69 data, and we computed the associated currents normalized vorticity (see Figure 1).

Figure 1: Reference data: on the left and middle panels, the SSH and SSC velocity (colored by the magnitude, with arrows giving the direction) simulated by NEMO; on the right, the corresponding normalized vorticity.

Using the SSH, `jaxparrow` can first estimate the geostrophic currents (Equation 1). As geostrophy is a major mechanism governing ocean dynamics, the vorticity derived from those currents present an overall similarity with the one obtain from NEMO data. However, we can clearly identify irregular areas (around (-4, 35.5), (-3, 36), and (-2.5, 35.5) in (longitude, latitude) coordinates, see Figure 2) where the geostrophic balance fails to capture the true ocean circulation.
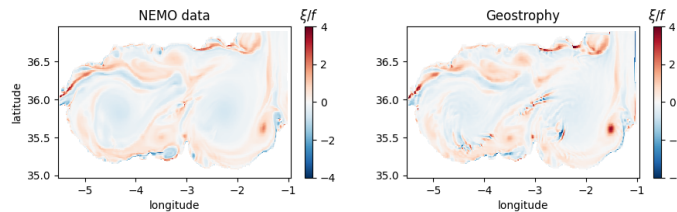

Figure 2: The qualitative comparison between reference (left panel) and geostrophic (right panel) normalized vorticities reveals several regions with highly erroneous estimations.

Starting from geostrophic currents, `jaxparrow` solves the variational formulation of the cyclogeostrophy (Equation 4), using in this example the classical gradient descent (Kantorovich & Akilov, 2016). As a result, almost all the problematic areas are now much more accurately reconstructed, leaving only costal or domain boundary regions with large differences from our reference vorticity (see Figure 3, left and middle panels). By evaluating the cyclogeostrophic disequilibrium (the functional J from Equation 4) along the optimization process, we clearly see that `jaxparrow` is able to close the cyclogeostrophic balance (right panel of Figure 3).
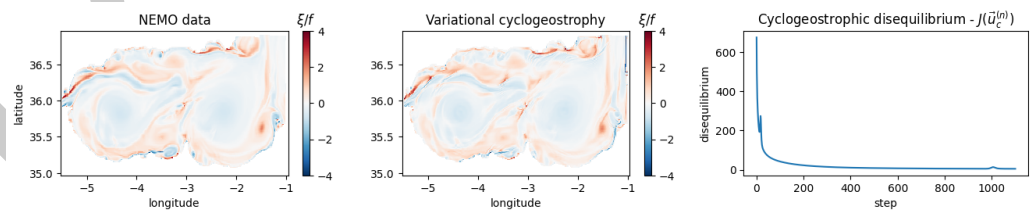

Figure 3: In contrast to the geostrophic approximation, variational cyclogeostrophy (middle panel) provide accurate reconstruction of the reference (left panel) normalized vorticities in all the inside of the domain. The right panel demonstrates the fast convergence towards cyclogeostrophic balance.

In comparison, `jaxparrow` can also estimate the cyclogeostrophic currents using the iterative scheme (Equation 3). In this example, it is evident that the point by point update of the velocities is not able to fill the cyclogeostrophic balance, and we notice that this estimation is qualitatively worse than the geostrophy (left and middle panels of Figure 4). Even with an

87 additional ad-hod threshold imposed on the residuals at the first iteration, divergence from
88 cyclogeostrophic equilibrium immediately occurs (see Figure 4, right panel).
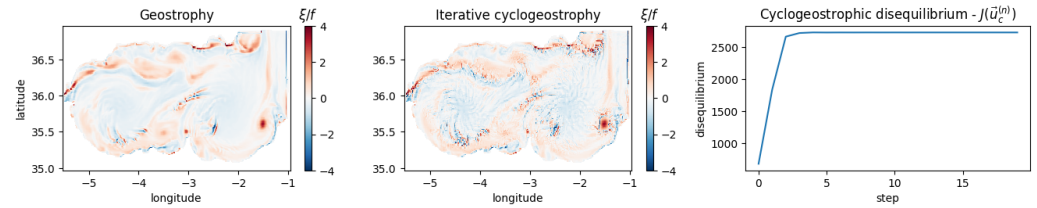

Figure 4: As exhibited in the right panel, the iterative approach diverges from the cyclogeostrophic balance; and we can notice from the two other panels that the resulting vorticity is qualitatively worse than the geostrophic one.

89 Those qualitative observations are inline with the quantitative evaluation we performed. We
90 computed the 1000 first percentiles of the vorticity distributions, and we observe, via a Q-Q
91 plot (Wilk & Gnanadesikan, 1968), that the percentiles of the variational distribution are the
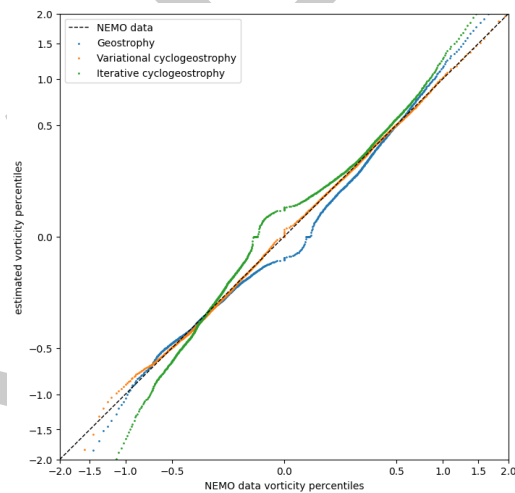92 closest to the ones of the reference distribution (Figure 5).

Figure 5: The percentiles of the normalized vorticity distributions demonstrate that our variational estimation of the cyclogeostrophy (in orange) corrects the tendency of the geostrophy (in blue) to over-estimate positive normalized vorticities, while the iterative scheme (in green) diverges and systematically overestimate the absolute normalized vorticity.

Availability

94 Beside the novel variational formulation, `jaxparrow` also offers the first to our knowledge open
95 implementation of the cyclogeostrophy resolution. The code is available on GitHub, with
96 the specific tag `joss` for the version matching this publication; and the documentation, with
97 pip-installation instuctions, usage examples, and toy notebooks, is hosted on Read the Docs.

Acknowledgements

References

Arnason, G., Haltiner, G., & Frawley, M. (1962). Higher-order geostrophic wind approximations. *Monthly Weather Review*, *90*(5), 175–185. https://doi.org/https://doi.org/10.1175/1520-0493(1962)090%3C0175:HGWA%3E2.0.CO;2

Bakun, A. (2006). Fronts and eddies as key structures in the habitat of marine fish larvae: Opportunity, adaptive response and competitive advantage. *Scientia Marina*, *70*(S2), 105–122. https://doi.org/https://doi.org/10.3989/scimar.2006.70s2105

Bradbury, J., Frostig, R., Hawkins, P., Johnson, M. J., Leary, C., Maclaurin, D., Necula, G., Paszke, A., VanderPlas, J., Wanderman-Milne, S., & others. (2021). JAX: Autograd and XLA. *Astrophysics Source Code Library*, ascl–2111. https://github.com/google/jax

Brodeau, L., Sommer, J. L., & Albert, A. (2020). *ocean-next/eNATL60: Material describing the set-up and the assessment of NEMO-eNATL60 simulations* (Version v1). Zenodo. https://doi.org/10.5281/zenodo.4032732

Cao, Y., Dong, C., Stegner, A., Bethel, B. J., Li, C., Dong, J., Lü, H., & Yang, J. (2023). Global sea surface cyclogeostrophic currents derived from satellite altimetry data. *Journal of Geophysical Research: Oceans*, *128*(1), e2022JC019357. https://doi.org/https://doi.org/10.1029/2022JC019357

Charney, J. G. (1955). The gulf stream as an inertial boundary layer. *Proceedings of the National Academy of Sciences*, *41*(10), 731–740. https://doi.org/https://doi.org/10.1073/pnas.41.10.731

Endlich, R. M. (1961). Computation and uses of gradient winds. *Monthly Weather Review*, *89*(6), 187–191. https://doi.org/https://doi.org/10.1175/1520-0493(1961)089%3C0187:CAUOGW%3E2.0.CO;2

Ioannou, A., Stegner, A., Tuel, A., LeVu, B., Dumas, F., & Speich, S. (2019). Cyclostrophic corrections of AVISO/DUACS surface velocities and its application to mesoscale eddies in the mediterranean sea. *Journal of Geophysical Research: Oceans*, *124*(12), 8913–8932. https://doi.org/https://doi.org/10.1029/2019JC015031

Kantorovich, L. V., & Akilov, G. P. (2016). *Functional analysis*. Elsevier.

Madec, G., Bourdallé-Badie, R., Chanut, J., Clementi, E., Coward, A., Ethé, C., Iovino, D., Lea, D., Lévy, C., Lovato, T., Martin, N., Masson, S., Mocavero, S., Rousset, C., Storkey, D., Müeller, S., Nurser, G., Bell, M., Samson, G., … Moulin, A. (2022). *NEMO ocean engine* (Version v4.2). Zenodo. https://doi.org/10.5281/zenodo.6334656

Maximenko, N., & Niiler, P. (2006). Mean surface circulation of the global ocean inferred from satellite altimeter and drifter data. *Proceeding of the Symposium on 15 Years of Progress in Radar Altimetry, Eur. Space Agency Spec. Publ., ESA SP*, *614*. https://citeseerx.ist.psu.edu/document?repid=rep1&type=pdf&doi=3a37ef4ad98374b642a360e1445474bb2bdcafed

Penven, P., Halo, I., Pous, S., & Marié, L. (2014). Cyclogeostrophic balance in the mozambique channel. *Journal of Geophysical Research: Oceans*, *119*(2), 1054–1067. https://doi.org/https://doi.org/10.1002/2013JC009528

Uchida, T., Le Sommer, J., Stern, C., Abernathey, R. P., Holdgraf, C., Albert, A., Brodeau, L., Chassignet, E. P., Xu, X., Gula, J., & others. (2022). Cloud-based framework for inter-comparing submesoscale-permitting realistic ocean models. *Geoscientific Model Development*, *15*(14), 5829–5856. https://doi.org/https://doi.org/10.5194/gmd-15-5829-2022

143 Wilk, M. B., & Gnanadesikan, R. (1968). Probability plotting methods for the analysis for
144 the analysis of data. *Biometrika*, *55*(1), 1–17. https://doi.org/https://doi.org/10.1093/
145 biomet/55.1.1